

C.-R. Lin
W.-J. Chen

The links-nodes-blobs model for shear-thinning-yield-stress fluids

Received: 22 March 1999
Accepted in revised form: 1 June 1999

C.-R. Lin (✉)
Materials Research Laboratories
Industrial Technology Research Institute
Chutung, Hsinchu 31015, Taiwan, R.O.C

W.-J. Chen
Department of Chemical Engineering
National Taipei University of Technology
Taipei 10643, Taiwan, R.O.C

Abstract A new model based on fractal and percolation concepts is proposed to explain the rheological behavior of shear-thinning yield-stress fluids. Suspension particles of the fluids are described in terms of the links-nodes-blobs (L-N-B) model. The complex suspension rheology can be interpreted via the similarity of the L-N-B model to the Rouse chain model. Consequently, the empirically universal relationship between the dimensionless shear stress, T , and the dimensionless shear rate, Γ , which was recently suggested by Coussot as $T = 1 + K\Gamma^n$ at $\Gamma < 0.3$ and approaches Newtonian behavior at $\Gamma > 50$, can be derived in terms of microscopic properties of a suspension of the force-free particles, fractal dimensions of the percolation system, and the critical lengths of the percolation system.

According to our study, a more precise and more general universal relationship, which fits experimental data well over a wide range from $\Gamma = 10^{-7}$ – 10^3 , is proposed as $T = 1 + \Gamma + K\Gamma^n$. The parameter K in the universal equation can be expressed as a function of the dimensionless cross-section of the blobs, the distribution of links, and fractal dimensions of the percolation system, while the exponent n in the universal equation is a function of the fractal dimensions only. The transition point of a shear-thinning yield-stress fluid from shear-thinning to Newtonian behavior was explicitly interpreted.

Key words Links-nodes-blobs model · Suspension rheology · Fractal scaling · Percolation

Introduction

Suspensions of mud, clays, coal slurries, and some polymer emulsions are non-Newtonian fluids exhibiting shear-thinning yield-stress behavior [1–3]. A yield stress, τ_c , needs to be overcome for the fluid to flow, and the apparent viscosity of these fluids decreases with increasing shear rate. This shear-thinning yield-stress behavior is attributed to the breakdown of the weak network bonding in suspensions. Conventionally, the flow curves of these non-Newtonian fluids are empirically fitted with the Bingham fluid model or more precisely with the Herschel–Bulkley model for the low-shear-rate data. Recently, the results of Coussot [4] showed that

structural similarity exists in clay–water suspensions over a wide solid content range in the laminar flow region with high values of the Peclet number. According to the Coussot's experimental results as shown in Fig. 1, all the flow curve data for clay–water suspensions of different volume fractions follow a master curve in a dimensionless (Γ , T) diagram as shown in Fig. 2. In this regard, dimensionless shear rate, $\Gamma = \eta_s \dot{\gamma} / \tau_c$, and dimensionless shear stress, $T = \tau / \tau_c$, are proposed, where $\dot{\gamma}$ is the shear rate, τ is the shear stress, and η_s is the viscosity of the corresponding suspension of force-free particles. At $\Gamma < 0.3$, the master curve represents a shear-thinning yield-stress behavior which can be expressed as

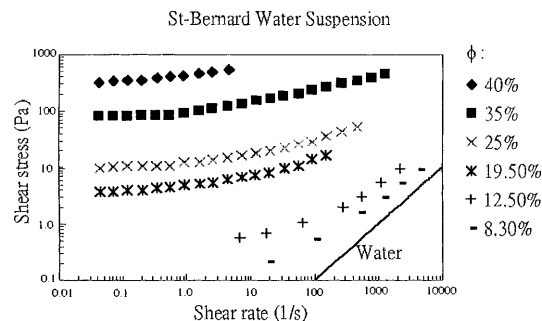


Fig. 1 Rheological data for St-Bernard sample–water suspensions of different solid fractions, and the flow curve of water (solid line) measured at 20 °C (taken from Ref. [4])

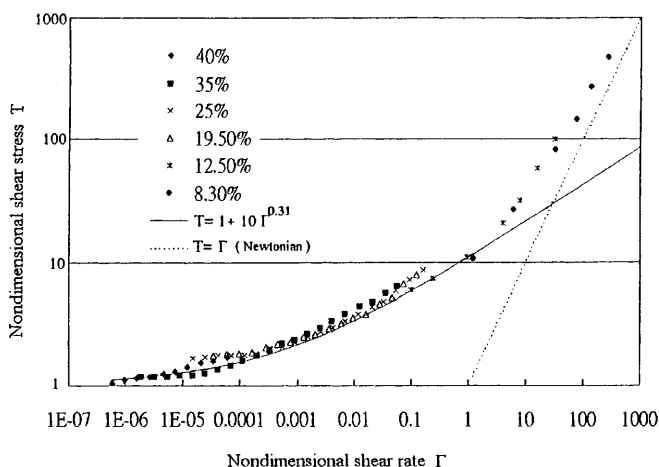


Fig. 2 The dimensionless shear rate and shear stress (Γ , T) diagram of St-Bernard sample–water suspensions. The data are the same as those in Fig. 1. According to the result of Coussot's simulation [4], the experimental data in the region of $\Gamma < 0.3$ are fitted with Eq. (1) by selecting $K = 10$ and $n = 0.31$, respectively

$$T = 1 + K\Gamma^n \quad (1)$$

Here K and n are material parameters which depend on characteristic times of the rupture and restoration processes, respectively. At $\Gamma > 50$, the master curve represents a Newtonian behavior, and the particles of the suspension are separately dispersed in the fluid. The dispersed particles in suspensions do not break down further at much higher shear rates. In fact, the viscous drag, which overwhelms the Brownian motion in the laminar flow region with high values of the Peclet number, dominates the segregation of particle aggregates in the suspension [2, 4]. Owing to the complexity of the suspension rheology, no strictly theoretical model for describing this non-Newtonian behavior has been satisfactorily developed.

A particle-filled suspension with a very low solid concentration acts as a form of separate particles dispersed in the fluid. As the solid content increases,

the interparticle interactions, such as the van der Waals force make separate particles form aggregates in the fluid. As solid content increases further, a tenuous suspension network forms, and the fluid exhibits a shear-thinning yield-stress behavior. The microstructure of these suspensions is similar to that of carbon-black filled rubber. It has been well documented in the literature that as the filler volume content, ϕ , is greater than the critical volume content, ϕ_c , carbon black exists as a continuous networklike agglomerate structure. The dynamic moduli of carbon-black filled rubber materials are strongly strain-dependent [5, 6]. As the strain amplitude increases to be higher than an apparent strain ε_{app} , the network structure of the carbon-black filled rubber system starts to break down. Concurrently, the storage modulus decreases monotonically while the loss modulus shows a peak, as a function of the strain amplitude. This nonlinear dynamic behavior is also known as the Payne effect. In the recent theoretical developments by Lin and Lee [7, 8], the Payne effect was successfully presented with the links-nodes-blobs (L-N-B) model. In this work, it was demonstrated that the L-N-B model can be applied to interpret the rheology of shear-thinning yield-stress fluids. Notably these two similar systems both exhibit the phenomenon of structural breakdown under deformation; however, the main difference between them is that the carbon-black filled rubber showing the Payne effect is subjected to a periodically sinusoidal vibration, while the shear-thinning yield-stress fluids in the present study are under deformation in a steady-shear flow.

The L-N-B model

According to Lin and Lee's model, as shown in Fig. 3, the filler's network structure in the static state can be described with the L-N-B model [9, 10]. The blobs are randomly connected as an infinite network through singly connected bonds (SCBs) (links) between the blobs. During the progress of deformation, the blobs are assumed to be entirely rigid so that they are not deformed; however, the links are deformed under tension, bending and/or torsion. The links even tend to break off when some failure strain is attained. A blob can be a dense suspension particle, a primary aggregate of colloids, or a cluster formed by coagulation of primary aggregates. The smallest-sized blobs correspond to a dense particle or a primary aggregate. The links correspond to tenuous network bonding between dense filler aggregates. The smallest link corresponds to a direct contact bonding between two dense particles or between two filler aggregates. The chains made of links and blobs are denoted as L-N-B chains. The connected points among L-N-B chains are called nodes. The average length of an L-N-B chain between two nearest

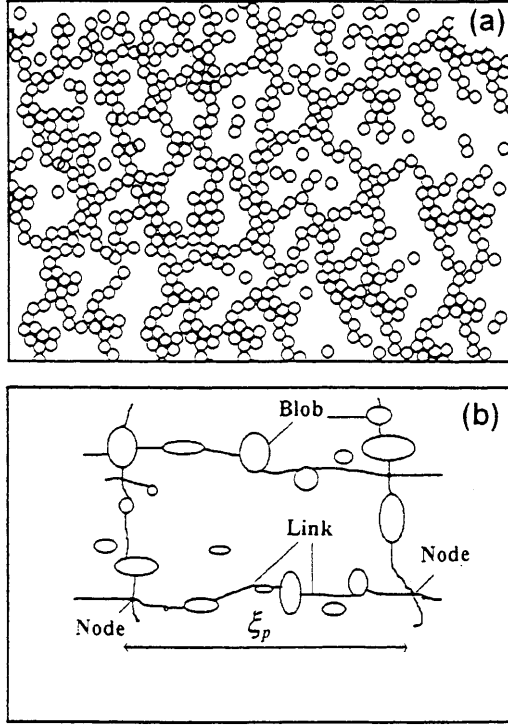


Fig. 3 Schematic plots of **a** the filler's network structure, and **b** the equivalent links-nodes-blobs (L-N-B) model (taken from Ref. [7]). The blobs correspond to dense filler aggregates that are not deformed throughout the whole deformation process; a blob can be a dense suspension particle, a primary aggregate of colloids, or a cluster formed by coagulation of primary aggregates. The smallest size of a blob is that of a dense suspension particle or a primary aggregate. The links correspond to tenuous filler bonding between dense filler aggregates. The smallest link corresponds to a direct contact bonding between two dense suspension particles or between two filler aggregates. The chains made of links and blobs are called L-N-B chains. The connected points among L-N-B chains are called nodes. The average length of an L-N-B chain between two nearest nodes is defined as ξ_p

nodes is defined as ξ_p . Macroscopically, for a length greater than ξ_p , the system is uniform; however, for a length shorter than ξ_p , an L-N-B chain is not necessarily formed. Hence, ξ_p corresponds to the critical length of a percolation system. ξ_p is finite as the filler volume content, ϕ , is greater than the critical volume content, ϕ_c , and ξ_p approaches infinity as $\phi \rightarrow \phi_c$. Based on the Kantor and Webman Hamiltonian [11], Lin and Lee [7, 8] have proven that

$$k_s(L_1) = \left(\frac{ma^2}{2d\bar{G}} + \frac{a^2}{dQ} \right)^{-1} \frac{1}{L_1} \quad (2)$$

$$\varepsilon_s(L_1) = \left(\frac{mL_1Q}{2d\bar{G}} + \frac{L_1}{d} \right) \varepsilon_b, \quad (3)$$

where $k_s(L_1)$ is the average force constant of an L-N-B chain with L_1 SCBs; $\varepsilon_s(L_1)$ and ε_b denote the failure strain of the L-N-B chain and that of an SCB,

respectively. \bar{G} and Q are local elastic constants corresponding to the change of angles between SCBs and the longitudinal deformation of an SCB, respectively; \bar{G} is controlled by the matrix around fillers, and Q is controlled by the van der Waals force between fillers. The length of an SCB is a . The Euclidean dimension of the percolation system is d . The average number of SCBs between two blobs is denoted by m . Moreover, the macroscopic stiffness of the percolation system, k_e , can be correlated to the microscopic force constant $k_s(L_1)$ by

$$\begin{aligned} k_e &= \xi_p^{2-d} \int_{L_1=1}^{\infty} f_1(L_1) k_s(L_1) dL_1 \\ &= \xi_p^{2-d} \left(\frac{ma^2}{2d\bar{G}} + \frac{a^2}{dQ} \right)^{-1} \frac{1}{\langle L_1 \rangle}, \end{aligned} \quad (4)$$

where $f_1(L_1)$ is the density distribution function of the number L_1 of SCBs in the L-N-B chain with $\int_{L_1=1}^{\infty} f_1(L_1) dL_1 = 1$, ξ_p^{2-d} correlates to the size of the unit cell, and $\langle L_1 \rangle$ is the harmonic average number of SCBs in the L-N-B chain, i.e.,

$$\langle L_1 \rangle = \left(\int_{L_1=1}^{\infty} \frac{f_1(L_1)}{L_1} dL_1 \right)^{-1}. \quad (5)$$

$\varepsilon_s(L_1 = 1)$ in Eq. (3) is defined as the apparent yield strain, ε_{app} . Once macroscopic strain is greater than ε_{app} , the filler network system starts to break down. Therefore, from Eqs. (3) and (4), the apparent yield stress of the percolation system, τ_c , can be expressed as

$$\tau_c = k_e \varepsilon_{app} = \xi_p^{2-d} \frac{Q\varepsilon_b}{a^2} \frac{1}{\langle L_1 \rangle}, \quad (6)$$

where $Q\varepsilon_b/a^2$ is the failure stress of an SCB bond, and $\langle L_1 \rangle$ is controlled by the L-N-B chain distribution in a unit cell.

For a suspension, with a particle volume content $\phi \geq \phi_c$, under simple shear deformation, the original suspension network structure breaks down as shear stress $\tau \geq \tau_c$, and the suspension starts to flow. During the breakdown process, the critical length of the percolation system, ξ_p , increases from a finite value to infinity in the initial unsteady state, and then ξ_p goes down to a finite value as a steady-shear-flow condition is attained. In order to distinguish the critical length of a suspension system at static conditions from that under steady simple-shear-flow conditions, the former is still represented as ξ_p (Fig. 4a), while the latter is written as ξ_g (Fig. 4b). According to the original definition of the L-N-B model [9, 10], there exists only one L-N-B chain in the repeated unit cell of size ξ_p ; however, for a suspension under steady simple shear flow, there may exist a group of broken L-N-B chain segments with different SCBs in a repeated unit cell of size ξ_g (Fig. 4b). Moreover, the size of ξ_g decreases as the shear rate, $\dot{\gamma}$, increases, and finally approaches a constant value as all L-N-B chains are broken into blobs.

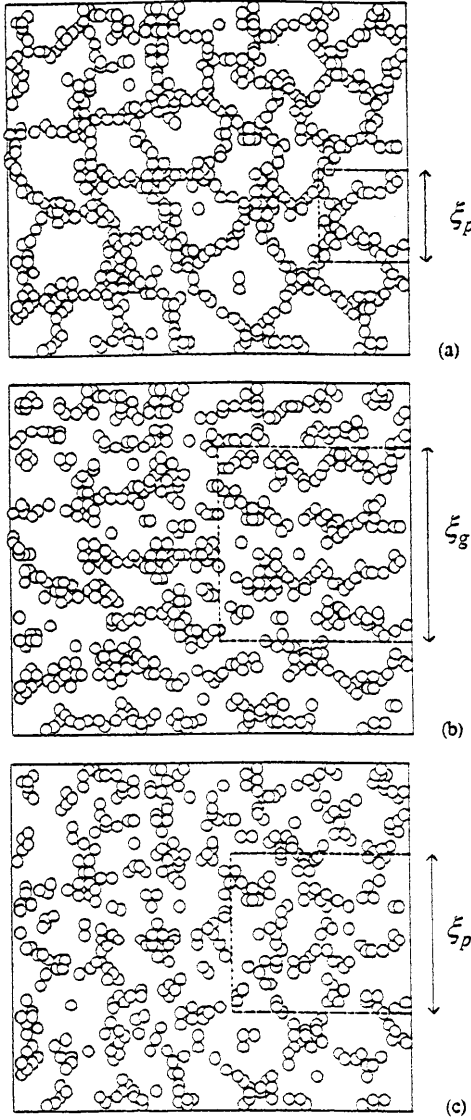


Fig. 4 The critical lengths of suspension systems with **a** a suspension particle volume content $\phi \geq \phi_c$ in the static state (a continuous suspension network formed), **b** a suspension particle volume content $\phi \geq \phi_c$ in the steady-shear-flow state (the continuous suspension network broken down), and **c** a suspension particle volume content $\phi < \phi_c$ in the static state (no continuous network formed)

For a suspension system with a particle volume content $\phi < \phi_c$, no continuous filler network forms in the fluid (Fig. 4c). Similar to a suspension with $\phi \geq \phi_c$ under steady simple shear flow, there may exist a group of L-N-B chain segments with different SCBs in a repeated unit cell of size ξ_p .

Fractal similarity between the Rouse chain fluid and the L-N-B chain fluid

The rheology of an L-N-B chain fluid is too complex to be solved analytically; however, the L-N-B chain fluid

model can be correlated to the Rouse chain fluid model through their fractal similarity [12–14]. For example, a fractal aggregate of size R formed by the number N of random agglomerated particles having the particle diameter a , obeys the following relationship [14]:

$$N = \alpha_1 \left(\frac{R}{a} \right)^{D_{m1}}, \quad (7)$$

where α_1 is a proportionality constant, and D_{m1} is the mass fractal dimension; $D_{m1} = 2.2 \sim 2.9$ for carbon black and $D_{m1} = 2$ for a Rouse chain.

For a dilute Rouse chain polymer solution under simple shear-flow conditions [15], the average value of the squared end-to-end length of a Rouse chain, $\langle r^2 \rangle$, can be correlated to the shear rate, $\dot{\gamma}$, as follows:

$$\frac{\langle r^2 \rangle}{\langle r^2 \rangle_{eq}} = 1 + \frac{1}{45} N(N+1)(N^2+1) \left(\frac{\xi_0}{H} \right)^2 \dot{\gamma}^2, \quad (8)$$

where $\langle r^2 \rangle_{eq}$ is $\langle r^2 \rangle$ in the static condition, N is the number of beads in a Rouse chain, ξ_0 is the friction coefficient of a bead, and H is the spring constant of a spring in a Rouse chain, respectively. Therefore, for large N , the strain of Rouse chains $\varepsilon \approx \frac{\langle r^2 \rangle^{0.5}}{\langle r^2 \rangle_{eq}^{0.5}} - 1 \approx N^2 \frac{\xi_0}{H} \dot{\gamma}$. In analogy to the Rouse chain, blobs in an L-N-B chain like beads in the Rouse chain are exerted all drag force by the fluid. Therefore, in this situation, the strain of L-N-B chains with L_1 SCBs is proposed to be

$$\varepsilon(L_1) = L_1^{D_a} \cdot \frac{\xi_0}{H_{L-N-B}} \dot{\gamma}, \quad (9)$$

where H_{L-N-B} is the force constant between two connected blobs, $H_{L-N-B} \approx k_s(L_1 = m)$, and D_a is a fractal dimension ($D_a = 2$ for the Rouse chain system). The spring constant, H , of the Rouse model is of entropic origin, and it is proportional to the absolute temperature [16], while the force constant of the L-N-B model is controlled by the local elastic constant, \bar{G} , of the matrix around fillers and by the van der Waals force constant, Q , between fillers, as given in Eq. (2). The temperature dependence of the force constant has been discussed by Lin and Lee [8].

According to Eq. (3), an L-N-B chain with L_1 SCBs will break off if the strain $\varepsilon > \varepsilon_s(L_1)$. Therefore, when the simple shear-flow system is driven at a shear rate of $\dot{\gamma}$, from Eqs. (3) and (9), all the L-N-B chains in the unit cell of size ξ_g obey: $L_1^{D_a} \cdot \frac{\xi_0}{H_{L-N-B}} \dot{\gamma} < \left[\frac{mL_1Q}{2d\bar{G}} + \frac{L_1}{d} \right] \varepsilon_b$; therefore, the maximum size, L_γ , of L-N-B chains in the unit cell is written as

$$L_\gamma = \left(\frac{Q\varepsilon_b}{ma^2} \xi_0^{-1} \dot{\gamma}^{-1} \right)^{\frac{1}{D_a-1}}. \quad (10)$$

According to Ferry [16], the viscosity, η , of the Rouse chain polymer solution can be expressed as

$$\eta = \eta_0 + \eta_1 a_R^2 N^2 \frac{\xi_0}{36}, \quad (11)$$

where η_0 is the viscosity of the solvent, η_1 is the number of Rouse chains in a unit volume, and a_R is the bead-to-bead length between two connected beads in a Rouse chain. N and ξ_0 are defined in Eq. (8). The second term on the right-hand side of Eq. (11) is attributed to the Rouse chains. Furthermore, if all the Rouse chains are broken down into separated beads suspended in the fluid, the viscosity, η_s , of the corresponding suspension of the force-free particles can be written as

$$\eta_s \approx \eta_0 + n_T a_R^2 \frac{\xi_0}{36}, \quad (12)$$

where n_T is the apparent density of beads in the fluid. Then, Eq. (11) can be rewritten as

$$\eta \approx \eta_s + a_R^2 \frac{\xi_0}{36} (n_1 N^2 - n_T), \quad (13)$$

In analogy to the Rouse chain system, the average viscosity in a repeated unit cell of size ξ_g of an L-N-B chain system can be expressed as

$$\eta \approx \eta_s + \xi_g^{-d} a_L^2 \frac{\xi_0}{36} (\Sigma_1 - \Sigma_2), \quad (14)$$

where

$$\Sigma_1 \begin{cases} \sum_{L_1=1}^{L_\gamma} g_1(L_1, \dot{\gamma}) L_1^{D_a} & \text{for } L_\gamma \geq 1 \\ \Sigma_2 & \text{for } L_\gamma < 1 \end{cases}, \quad (15)$$

$$\Sigma_2 = \sum_{L_1=0}^{L_\gamma} g_1(L_1, \dot{\gamma}) (L_1 + 1)^{D_b}. \quad (16)$$

In these expressions, D_a is defined in Eq. (9), D_b is a fractal dimension which correlates the number of blobs, n_B , in an L-N-B chain to the number of SCBs of the L-N-B chain $n_B(L_1) \approx (L_1 + 1)^{D_b}$, and $D_b = 1$ for the Rouse system), a_L is the blob-to-blob length between two connected blobs, $g_1(L_1, \dot{\gamma})$ is the number of L-N-B chains with L_1 SCBs in the repeated unit cell under a shear rate $\dot{\gamma}$, and η_s is the viscosity of the corresponding suspension of force-free particles. Σ_1 corresponds to the sum of the squared radii of the L-N-B chains in the repeated unit cell of size ξ_g . In addition to this, Σ_2 is the number of blobs in the repeated unit cell. Since the average properties in the repeated unit cells with dimension greater than or equal to ξ_g are uniform for a percolation system, the apparent blob density, n_T , defined in Eq. (12) can be expressed as

$$n_T = \xi_g^{-d} \Sigma_2. \quad (17)$$

To combine Eqs. (14) and (17), the viscosity of an L-N-B chain system can be simplified as follows:

$$\eta \approx \eta_s + n_T a_L^2 \frac{\xi_0}{36} \left(\frac{\Sigma_1}{\Sigma_2} - 1 \right). \quad (18)$$

The universal relationship between shear stress and shear rate

The contribution of viscous force of the L-N-B chain fluid to the shear stress, τ , of flow is equal to the product of the viscosity, η , and the shear rate, $\dot{\gamma}$. The flow of a shear-thinning yield-stress fluid happens at a shear stress $\tau \geq \tau_c$, and moreover, the shear stress builds up with increasing shear rate. Under such circumstances, the contribution of both the viscous force of the L-N-B chain fluid and the elastic force of the tenuous network structure to the shear stress of flow are assumed to be additive, i.e., $\tau = \tau_c + \eta \dot{\gamma}$. Therefore, the contribution of the viscous force of the L-N-B chain fluid to the dimensionless shear stress, τ/τ_c , is given by using Eq. (18) as follows:

$$\frac{\tau - \tau_c}{\tau_c} = \frac{\eta \dot{\gamma}}{\tau_c} \approx \frac{\eta_s \dot{\gamma}}{\tau_c} + \frac{n_T a_L^2 \frac{\xi_0}{36} \dot{\gamma}}{\tau_c} \left(\frac{\Sigma_1}{\Sigma_2} - 1 \right), \quad (19)$$

where the dimensionless drag stress $(n_T a_L^2 \frac{\xi_0}{36} \dot{\gamma})/\tau_c$ corresponds to the ratio of the stress generated from the drag force on separated blobs to the critical yield stress. According to percolation theory, Σ_1/Σ_2 corresponds to an average squared radius and can be expressed as a scaling function in the form [10]

$$\frac{\Sigma_1}{\Sigma_2} = \xi_g^{-D_c} \Psi \left(\frac{L_\gamma}{\xi_g} \right) \propto \begin{cases} L_\gamma^{D_c} & \text{for } L_\gamma \gg 1 \\ 1 & \text{for } L_\gamma < 1 \end{cases}, \quad (20)$$

where Ψ is an arbitrary scaling function, L_γ is defined in Eq. (10), and D_c is a fractal dimension.

Since the viscosity, η_s , of suspensions of force-free particles is much larger than the solvent viscosity, η_0 , Eq. (12) reduces to $\eta_s \approx n_T a_R^2 \frac{\xi_0}{36}$, and the dimensionless drag stress $(n_T a_L^2 \frac{\xi_0}{36} \dot{\gamma})/\tau_c$, as defined in Eq. (19), reduces to

$$\frac{n_T a_L^2 \frac{\xi_0}{36} \dot{\gamma}}{\tau_c} \approx \frac{\eta_s \dot{\gamma}}{\tau_c} = \Gamma. \quad (21)$$

Moreover, from Eqs. (6) and (10), we have

$$(L_\gamma)^{D_c} \approx \left(\frac{n_T a_L^2}{36 \xi_p^{2-d}} \frac{\langle L_1 \rangle}{m} \Gamma^{-1} \right)^{\frac{D_c}{D_a-1}}, \quad (22)$$

where the dimensionless group $n_T a_L^2 / 36 \xi_p^{2-d}$ corresponds to the effective cross-sectional ratio of separated blobs in the unit cell, and $\langle L_1 \rangle / m$ is attributed to the L-N-B chain distribution, respectively. Equations (19), (20), and (22) prove that the shear-thinning yield-stress fluid systems obey a fractal scaling law in that the dimensionless shear stress, T , varies as a function of the dimensionless shear rate, Γ .

Under the condition that $L_\gamma \gg 1$, Eq. (20) reduces to $\frac{\Sigma_1}{\Sigma_2} = L_\gamma^{D_c}$, and Eq. (19) can be rewritten as

$$\begin{aligned} \frac{\tau - \tau_c}{\tau_c} &= \frac{\eta \dot{\gamma}}{\tau_c} \approx \frac{\eta_s \dot{\gamma}}{\tau_c} + \frac{n_T a_L^2 \frac{\xi_0}{36} \dot{\gamma}}{\tau_c} (L_\gamma^{D_c} - 1) \\ &\approx \frac{\eta_s \dot{\gamma}}{\tau_c} + \frac{n_T a_L^2 \frac{\xi_0}{36} \dot{\gamma}}{\tau_c} L_\gamma^{D_c} \end{aligned} \quad (23)$$

Combining Eqs. (21)–(23) yields the following universal relationship:

$$\begin{aligned} T = \frac{\tau}{\tau_c} &= 1 + \Gamma + \left(\frac{n_T a_L^2 \langle L_1 \rangle}{36 \xi_p^{2-d} m} \right)^{\frac{D_c}{D_a-1}} \Gamma^{\frac{D_a-D_c-1}{D_a-1}} \\ &= 1 + \Gamma + K \Gamma^n \end{aligned} \quad (24)$$

In these expressions, the parameter K in Eq. (24),

corresponding to $K = \left(\frac{n_T a_L^2 \langle L_1 \rangle}{36 \xi_p^{2-d} m} \right)^{\frac{D_c}{D_a-1}}$, is a function of

the dimensionless cross-section of the blobs, the distribution of links, and the fractal dimensions of the percolation system, as defined in Eq. (22); the exponent n in Eq. (24) is a function of the fractal dimensions as $n = \frac{D_a-D_c-1}{D_a-1}$.

The Coussot equation (Eq. 1), applicable at $\Gamma < 0.3$, is just a limiting case of the general universal equation (Eq. 24). According to Coussot simulation [4], n is about 0.2–0.3. In the region of $\Gamma < 0.3$, we have $\Gamma < K \Gamma^n$, and Eq. (24) reduces to Eq. (1). In order to test the applicability of the newly proposed universal relationship, the same experimental data by Coussot, as shown in Fig. 1, are fitted with Eq. (24) by using the same values of parameters K and n obtained from the Coussot's curve-fitting of Fig. 2, and our result is shown in Fig. 5 for comparison. It is found that our proposed universal equation in a modified form fits the data well over a wide range of dimensionless shear rates from $\Gamma = 10^{-7}$ – 10^3 .

At high shear rates such as $L_\gamma < 1$, all L-N-B chains in the fluid break down into separated blobs, the fluid becomes a Newtonian fluid, and Eq. (24) reduces to $T = \Gamma$. According to Eq. (22), such a transition occurs at $\Gamma \approx \frac{n_T a_L^2 \langle L_1 \rangle}{36 \xi_p^{2-d} m}$.

Conclusion

The breakdown of the weak network bonding in a suspension fluid has been described with the L-N-B

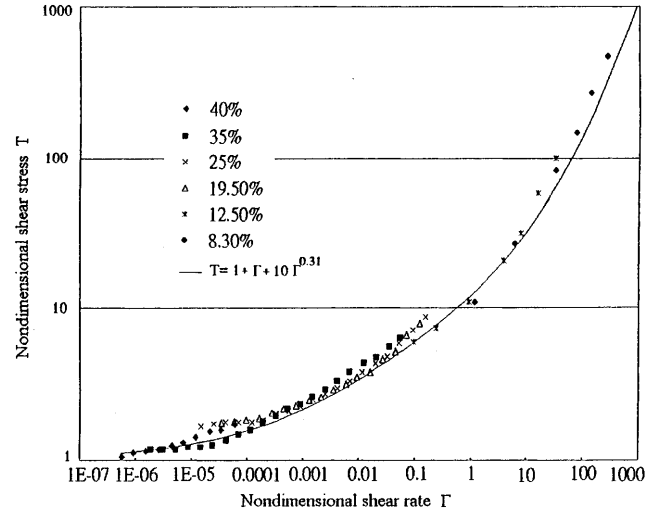


Fig. 5 The experimental data of St-Bernard sample–water suspensions which are the same as those in Fig. 2 and the fitting curve from Eq. (24) using $K = 10$ and $n = 0.31$

model. By using this model, the yield stress, τ_c , which needs to be overcome for the fluid to flow, corresponds to the stress that is required for the deformation of the L-N-B network structure to attain the apparent yield strain, ε_{app} . Instead of directly interpreting the complex rheology of an L-N-B chain fluid via solving the constitution equation of fluids, the fractal similarity between an L-N-B chain and a Rouse chain is applied for the microstructural study of the rheology of an L-N-B chain fluid. By using this new approach, we demonstrated that shear-thinning yield-stress fluids obey a fractal scaling law in that the dimensionless shear stress, T , varies as a function of the dimensionless shear rate Γ . Moreover, we proposed a universal equation in a modified form, $T = 1 + \Gamma + K \Gamma^n$. Coussot's model, which is applicable at $\Gamma < 0.3$, is just a limiting case of the newly proposed universal equation. The parameters K and n in the universal equation correspond to

$K = \left(\frac{n_T a_L^2 \langle L_1 \rangle}{36 \xi_p^{2-d} m} \right)^{\frac{D_c}{D_a-1}}$ and $n = \frac{D_a-D_c-1}{D_a-1}$, respectively. When

plotting the dimensionless shear stress as a function of the dimensionless shear rate, the transition of a shear-thinning yield-stress fluid from shear-thinning to Newtonian behavior is seen to occur at $\Gamma \approx \frac{n_T a_L^2 \langle L_1 \rangle}{36 \xi_p^{2-d} m}$.

References

1. Barnes HA, Hutton JF, Walters K (1989) An introduction to rheology, Elsevier, Amsterdam
2. Russel WB, Saville DA, Schowalter WR (1989) Colloidal dispersions. Cambridge University Press, Cambridge, pp 456–471
3. Coussot P, Piau JM (1994) *Rheol Acta* 33:175–184
4. Coussot P (1995) *Phys Rev Lett* 74:3971–3974
5. Payne AR (1965) In: Kraus G (ed) Reinforcement of elastomers. Wiley, New York, pp 69–123
6. Medalia AI (1978) *Rubber Chem Technol* 51: 437–523
7. Lin CR, Lee YD (1996) *Macromol Theory Simul* 5:1075–1104
8. Lin CR, Lee YD (1997) *Macromol Theory Simul* 6:339–350
9. Stanley HE (1977) *J Phys A* 10:L211–L220
10. Stauffer D, Aharony A (1992) Introduction to percolation theory, Taylor & Francis, London
11. Kantor Y, Webman I (1984) *Phys Rev Lett* 52:1891–1894
12. Mandelbrot BB (1982) The fractal geometry of nature. Freeman, San Francisco
13. Bunde A, Havlin S (1991) Fractals and disordered systems, Springer, Berlin Heidelberg, New York
14. Klüppel M, Heinrich G (1995) *Rubber Chem Technol* 68:623–651
15. Bird RB, Curtiss CF, Armstrong RC, Hassager O (1987) Dynamics of polymeric liquids, vol 2. Kinetic theory, Wiley, New York
16. Ferry JD (1980) Viscoelastic properties of polymers. Wiley, New York